PARTICULE OBŢINUTE DIN PRECURSORI DE SILICE PRIN METODA SOL-GEL – MATRICE ALE UNOR SONDE FLUORESCENTE DE PH

SOL-GEL OBTAINED SILICA BASED PARTICLES – SENSING PLATFORMS FOR FLUORESCENT PH PROBES

LIGIA TODAN[1] * , MARIANA VOICESCU[1], DANA C. CULIȚĂ[1], SIMONA PETRESCU[1], MARIA MAGANU[2], CRINU CIUCULESCU[2]

[1]"Ilie Murgulescu" Institute of Physical Chemistry, Romanian Academy, 202 Splaiul Independentei, 060021 Bucharest, Romania
[2]"Costin D. Nenițescu" Organic Chemistry Institute of the Romanian Academy, 202B Splaiul Independentei, 060023 Bucharest, Romania

Sol-gel obtained silica and organo silica particles, doped with rhodamine B (Rh B), with potential applications as sensing platforms for fluorescent pH probes were obtained. The silica matrices were generated by sol-gel method from different SiO_2 sources and using different routes: the aqueous one with colloidal silica as precursor and the alkoxide one starting with tetraethoxysilane (TEOS) as such and with different organic functionalities. The product was characterized from structural and compositional point of view (FTIR, UV-VIS, SEM, BET surface area and porosity). The leaching of the dye from the matrices was detected by GC-MS. The fluorescence properties and variation with pH were determined. Structural interconversions of the dye take place as a function of the matrices and pH which influence the maximum absorption and emission wavelength of RhB. The presence of organic substituents in TEOS generates a quenching of the RhB fluorescence.

S-au obţinut prin metoda sol-gel particule pe bază de silice şi de silice modificată organic, dopate cu rhodamină B (Rh B), cu potenţiale aplicaţii în obţinerea unor sonde fluorescente de detectare a pH-ului. Matricile de silice au fost generate prin metoda sol-gel din diverşi precursori de SiO_2, folosind rute diferite: ruta apoasă având ca precursor silicea coloidală şi ruta alcoxidică pornind de la tetraetoxisilan (TEOS) ca atare şi modificat organic. Produsul a fost caracterizat din punct de vedere structural şi compoziţional (FTIR, UV-VIS, SEM, aria suprafeţei BET şi porozitatea). Percolarea colorantului din matrice a fost detectată prin GC-MS. S-au determinat proprietăţile fluorescente şi variaţia lor cu pH-ul. Au loc interconversii structurale ale colorantului funcţie de matrice şi de pH, care influenţează lungimea de undă a maximului de absorbție și emisie a RhB. Prezenţa substituenţilor organici în TEOS generează stingerea fluorescenței RhB.

Keywords: *silica/organosilica particles, sol-gel, rhodamine B, fluorescent pH probes*

1. Introduction

Sol-gel derived materials offer many advantages when used as chemical receptor matrices due to the versatility of the sol-gel process with regard to the design of products for specific optical applications and to the relatively fast and easy steps in catalysis of alkoxides under room temperature [1, 2]. Silica represents one of the most studied sol-gel derived matrix used for entrapping sensor molecules due to its remarkable properties (transparency, stability, proton diffusion in case of pH sensor, etc) and the preparation of hybrid materials containing organic groups covalently bonded to polysiloxane allows an easy modification of silica network [3, 4].

Rhodamines are xanthene derivatives belonging to an important class of fluorescent laser dyes with a large field of applications as sensory material [5-9]. Rhodamine B can exist in three isomeric forms (lactone, zwitterion, cation) which have different optical properties and undergo an intrinsic equilibrium in solution, depending on the interaction with the analyte and is one of the principal species used as sensory material [5-8].

Different approaches to immobilize several pH indicators in a sol-gel silica matrix were undertaken and the influence of the method on the sensor's characteristics was reported [10].

The optical properties of Rhodamine 6G doped silica glasses, prepared by sol-gel method as photoluminescent homogeneous bulk disks and by grafting reactions, with the dye immobilized on silica gel modified with chemically bonded organic groups, were studied [11-13].

Most sol-gel based pH sensors are derived from tetraethoxysilane (TEOS) aerogel [3]. In order to increase the dye entrapment efficiency in sol-gel system, silane precursors bearing organic functional groups were incorporated in the reaction,

* Autor corespondent/*Corresponding author*,
E-mail: l_todan@yahoo.co.uk

introducing thus unhydrolizable groups in the silica network and generating the so-called ORMOSILs, versatile materials widely used for the development of sensors [1, 4]. A hybrid matrix which incorporated a chromophore was obtained by co-hydrolysis of tetraethoxysilane with functionalized alkoxides and films for photonic application were deposited [14,15].

The present work follows our previous study [16] and deals with photophysical and photochemical properties of fluorescent pH sensitive composite particles, obtained by encapsulating rhodamine B (Rh B) in silica matrices generated from different SiO_2 sources: colloidal silica and hybrid xerogels obtained from tetraethoxysilane (TEOS) and by co-condensation of TEOS with phenyltriethoxysilane (PhTEOS) and methyltriethoxysilane (MeTEOS). Both routes of the sol-gel method (the alkoxide and the aqueous one) have been used. The properties were determined in an aqueous environment. The results have relevance to potential applications as sensing platforms for fluorescent pH probes.

2. Experimental

2.1. Materials and sample preparation

All the reagents were purchased from commercial suppliers (Sigma-Aldrich, Merck, Riedel-de Haën). A Britton-Robinson buffer was prepared (H_3PO_4/ H_3BO_4/ acetic acid, equal volumes of a 0.04 mol L^{-1} solution each) and a 0.2 mol L^{-1} NaOH solution was used for titration.

The experiments were undertaken at room temperature. All the samples have been prepared under continuous stirring. First the alkoxides were solved in the corresponding quantity of alcohol (the molar ratio SiO_2/ ROH =1/6), respectively the colloidal silica was diluted with water, in order to ensure the same SiO_2 concentration in all samples.

Three alkoxide solutions in ethanol were prepared of the following precursors: TEOS, MeTEOS-TEOS (1:1 molar ratio) and PhTEOS-TEOS (1:1 molar ratio). 0.5 mL Rh B solution in methanol (10^{-4} molar) were added to each precursor solutions.

In case of the colloidal silica solution, a pH adjustment to a 6-7 value was undertaken with a 25 wt% HNO_3 solution before adding the dye and after 24 h at 50^0C the powder was obtained.

In case of the alkoxide solutions the required amount of water containing the acid or basic catalyst was added drop-wise (the molar ratio SiO_2/ H_2O =1/6). The hydrolysis took place in two consecutive steps: in the first step, an aqueous HCl solution was added until the pH of the mixture became acidic (pH ≈ 2). After two hours of stirring at room temperature, the pH was raised at ≈ 10 by adding aqueous NH_4OH solution. Gelation occured instantly for the TEOS sample, after 24 hours for the methyl derivative and 30 days later for the phenyl one. The samples were air-dried for 120 days and mixed from time to time so the final products were obtained as powders [16].

For fluorescence measurements, a quantity of each of the four powders was placed on filter paper lining some sieves and thus were immersed in solutions with variable pH: 2, 4.93, 8.19, 10 and 12, which were obtained by adding drop-wise NaOH solution to the Britton-Robinson buffer. The powders were kept there for about 15 minutes. After each immersion, the samples were dried at 80°C for an hour and then fluorescence measurements were undertaken.

2.2. Characterization techniques

The UV-Vis diffuse reflectance spectra were recorded using a spectrophotometer Perkin Elmer Lambda 35, equipped with an integrating sphere. As reference, a certified reflectance standard, spectralon, has been used and the measurements were carried out in the range 900-200 nm. The sample holder is 8º wedge with data interval, 1 nm; scan speed, 120 nm/min and slits, 4 nm.

Scanning electron microscopy (SEM) was performed with an Auriga model Carl Zeiss SMT workstation.

The specific surface area and pore characterization of the samples were determined by nitrogen adsorption at -196ºC on a Micromeritics ASAP 2020 automated gas sorption system. The samples were outgassed at 120ºC for 3 hours under vacuum prior to N_2 adsorption. Specific surface areas (S_{BET}) were calculated according to Brunauer-Emmett-Teller (BET) equation using adsorption data in the relative pressure range 0.05 and 0.30 while pore size distributions were derived from the desorption branch using the Barrett–Joyner–Halenda (BJH) model. The total pore volume (V_{total}) was estimated from the amount adsorbed at the relative pressure of 0.99.

FT-IR spectra were recorded on a Brucker Vertex 70 Spectrometer, with horizontal device for attenuated reflectance and diamond crystal, on a spectral window ranging from 4000 to 400 cm^{-1}, at a spectral resolution of 2 cm^{-1}. Spectra were recorded without any sample preparation and were processed with OPUS 5.5 program (Brucker).

The fluorescence emission and excitation spectra of RhB embedding powders were recorded with a Jasco FP-6500 Spectrofluorometer, using 1 nm bandpasses for the excitation and the emission monochromators, the detector response of 1 sec, the scan rate of 100 nm min^{-1}, data pitch of 0.5 -1 nm. The excitation and emission wavelengths were 510 and 600 nm, respectively.

pH values were measured with a digital certified pH meter (pH 315i, STD 61010A-1, Germany) at room temperature.

The leaching of Rh B from the matrices

was tested by determining its presence in the solution used for pH variation. This solution was analysed by gas chromatography coupled with mass spectrometry (GC-MS). The GC-MS analysis was carried out using an Agilent 6890N/5975 B equipment. A HP-5MS 5% phenylmethyl siloxane capillary column was used for the separation of the sample components. The injector functioned in the following mode: initial temperature 250°C, pressure 6.89 psi, split ratio 0.2 1^{-1}, split flow 0.2 mL min^{-1}, total flow 3.9 mL min^{-1}, gas saver - on, saver flow 20.0 mL min^{-1}, saver time 5 min, and gas type - helium. The column had the following characteristics: max. temperature 325°C, nominal length 30.0 m, nominal diameter 250.0 µm, nominal film thickness 0.25 µm, initial flow 1.0 mL min^{-1}, nominal initial pressure 6.89 psi, average velocity 36 cm s^{-1}, inlet - front inlet, outlet - MSD, and outlet pressure - vacuum. The mode of functioning was constant flow.

3. Results and Discussion

3.1.UV-VIS analysis

UV-VIS diffuse reflectance spectra of various as prepared Rh B-matrices (Fig. 1A) as well as of PhTEOS-TEOS-Rh B at pH 2 and 12 (Fig. 1B) showed the absorption band ~422 nm for TEOS-Rh B matrice, batochromic shifted at 440 nm for MeTEOS-TEOS-Rh B and at 462 nm for PhTEOS-TEOS-Rh B. The absorption bands appear at 578, 582 and 590 nm and are characteristic to the $n \rightarrow \pi^*$ and $\pi \rightarrow \pi^*$ electronic tranzitions of the Rh B. The batochromic shift, more pronunced for PhTEOS-TEOS matrix, is attributed to the structure of matrices in which Rh B is encapsulated where strong interactions are considered especially at pH 12. To compare, the absorption of colloidal SiO_2-Rh B matrix was performed, Fig. 1C**.** A pH dependend behavior of Rh B absorption in the SiO_2 matrice was observed. Hence, at pH 12, three absorption bands for Rh B in SiO_2 are observed: at 554, 586 and 644 nm. The appearance of the bands from 586 nm and 644 nm confirms that the carboxylic acid group of the Rh B reacts on the surface of SiO_2 through the anion form of Rh B ($Rh B^-$). Thus, the existence of the Rh B dimers as well as the molecular aggregation effect of Rh B in both colloidal SiO_2- and alkoxide matrices, are taken into account.

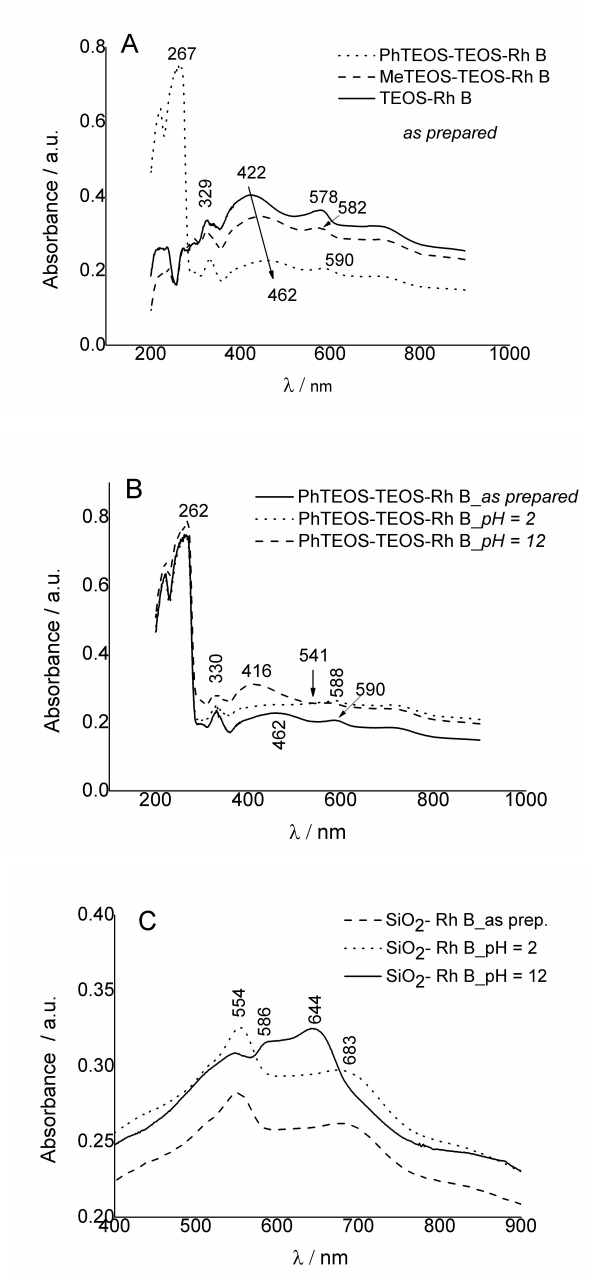

Fig. 1 - UV-Vis diffuse reflectance spectra of as prepared Rh B matrices (A), PhTEOS-TEOS-Rh B matrix at pH 2 and pH 12 (B) and SiO_2-Rh B matrix (C) / *Spectrele de reflectanţă difuză UV-Vis ale matricilor Rh B preparate ca atare (A), ale matricilor PhTEOS-TEOS-Rh B la pH 2 şi 12 (B) şi ale matricii SiO_2-Rh B (C)* .

3.2. Determination of BET surface area and porosity

The surface area and pore volume of colloidal silica-Rh B powder were determined by N_2 sorption analysis and the values were compared with the ones of the alkoxide matrices including the dye, previously presented in [16]. The results are shown in Table 1.

As can be seen, the specific surface area of the colloidal SiO_2 sample is smaller than the one of the alkoxide derived powders but the pore volume is about the same.

The silica matrix derived from PhTEOS-TEOS has a very small adsorption volume and has been considered as non-porous for this reason.

According to the pore size distribution curve, the mean pore diameter values are distinguished showing mesoporous structures in all cases. The pore topology makes a great contribution to the fluorescent properties because the space confinement can limit the freedom

Table 1

Specific surface area, pore volume and pore size of the colloidal silica and alkoxide matrices
Aria suprafeței specifice, volumul porilor şi dimensiunea porilor matricilor de silice coloidală şi alcoxidică

Sample/*Probă*	**S_{BET} (m^2 g^{-1})**	**V_{total} (cm^3 g^{-1})**	**Pore size (nm)/ *Dimensiunea porilor* (nm)**
colloidal SiO_2-Rh B	182	0.452	8.7
TEOS-Rh B*	488*	0.392*	3.2
MeTEOS-TEOS-Rh B*	798*	0.445*	2.2

Notă/Note: * [16]

Table 2

IR Main bands (cm^{-1}) for the materials obtained from colloidal silica embedding Rh B
Principalele benzi IR (cm^{-1}) pentru materialele obţinute din silice coloidală înglobând Rh B

Assignement / *Atribuire*	**Colloidal silica / *Silice coloidală***			
	a)	**b)**	**c)**	**references**
v (Si-)O-H)		3855	3855	[18]
v (Si-)O-H)			3410	[18, 19]
v (H-)O-H)$_{sym}$	3210			[18, 19]
v (C=O) in lactone Rh B			1783	[20]
v (C=N^+) and/or v $_{sym}$(COH)	1638	1654	1638	[20]
v (Si-O-(Si) $_{Asym}$	1067	1107	1073	[18, 19]
v (Si-O-H) $_{Asym}$	974	973		[18, 19]
v (Si-O(-Si)$_{sym}$	799	799	796	[19]
δ(Si-O-Si)	462	458	455	[18]

a) as prepared sample*/ proba preparată ca atare*; b) sample at pH 2 */ proba la pH 2;* c) *sample at pH 12 /* proba la pH 12
v_{sym}(COH) – symetric vibrations of cationic oxygen-containing heterocycle */vibraţii simetrice ale heterociclului conţinând oxigen cationic*

Table 3

IR main bands (cm^{-1}) for the materials obtained from different alkoxides embedding Rh B
Principalele benzi IR (cm^{-1}) pentru materialele obţinute din diferiţi alcoxizi înglobând Rh B

Assignement *Atribuire*	**Alk 1**			**Alk 2**			**Alk 3**		
	a)	**b)**	**c)**	**a)**	**b)**	**c)**	**a)**	**b)**	**c)**
O-H and C-H	~3000	~3000	~3000	~3000	~3000	~3000	~3000	~3000	~3000
v (C=O)	1742	1742	1742	1746	1746	1746		1740	1740
v $_{sym}$ (COH)	1629			1636					
v (Ar)							1590	1590	1590
v (C-Ar)	1372	1365	1365		1369	1369		1350	1350
v(Si-O- Si)$_{asym}$LO		1207	1207						
v(Si-O-Si)$_{asym}$TO	1055	1055	1055	1024	1037	1037	1033	1033	1033
v (Si-O(-Si)$_{sym}$	798	798	798	764	764	764	748	748	748
δ(Si-O-Si)	448	448	448	450	450	450	479	479	479

a) a) as prepared sample*/ proba preparată ca atare*; b) sample at pH 2 */ proba la pH 2;* c) sample at pH 12 / proba la pH 12
Alk 1- TEOS-Rh B; Alk 2- MeTEOS-TEOS-Rh B; Alk 3- PhTEOS-TEOS-RhB; v_{sym}(COH)– symetric vibrations of cationic oxygen-containing heterocycle */vibraţii simetrice ale heterociclului conţinând oxigen cationic;* Ar – aromatic ring */ ciclu aromatic*

degree of the dye molecule [9]. As shown in the UV-vis spectroscopic measurements, the difference in the pore size of the as prepared samples could contribute to the difference of the shifts of the absorption peaks.

3.3. FT-IR analysis

The four composite samples obtained from colloidal silica and different alkoxides embedding Rh B were analyzed by IR spectroscopy following their evolution in an acid and basic environment. The main bands are identified and presented in Table 2 and respectively Table 3.

According to the data in Table 2, the 3000-3800 cm^{-1} wavenumber region exhibits bands characteristic for the streching modes of hydroxyl groups. The bands at lower wavenumbers (~ 3200-3500 cm^{-1}) can be due to the –OH streching mode of adsorbed water (as prepared sample) [17,18]. At higher wavenumbers (3600 - 3800 cm^{-1}) bands associated with the streching modes of hydrogen bonds with the silanol groups appear (the pH 2 and pH 12 samples) [17]. The region characteristic of silica structure is located in the 1200-700 cm^{-1} range: bands associated with Si-O-Si streching mode and Si-OH bond streching [17,18].

The presence of rhodamine B could be infered by the presence of the shoulder at 1783 cm^{-1} for the pH 12 powder attributed to the lactone form of Rh B [19]. The lactone form of Rh B is colorless, the loss of the pink shade of the powders being thus explained [5, 6, 8]. The peaks at 1640-1650 cm^{-1}, characteristic for rhodamine cations (HR^+), correspond to vibrations of the cationic oxygen-containing heterocycle [19]. Moreover, the vibrations in the 1640 cm^{-1} region can also be assigned to v (C=N^+) considering the delocalization of charge in the carbonium cation [19].

When Rh B is embedded in colloidal silica, one can assume that the dye is a mixture of tautomers, at an acid pH the cationic form of Rh B

is predominant while at a basic pH a partial conversion to the lactone form takes place.

According to Table 3, all three alkoxide matrices show absorption bands in the high-frequency (3700-2700 cm^{-1}) region of the spectrum which are usually associated with O-H and C-H streching modes, groups found in both matrices and dye [15, 20-22]. In the 2000-1200 cm^{-1} range characteristic peaks for rhodamine B can be identified: vibrations of C=O in the carboxyl group at ~1740 cm^{-1}, symetric vibrations of cationic oxygen-containing heterocycle, at 1630-1640 cm^{-1}, vibrations of aromatic rings polarized by charge at 1584-1600 cm^{-1} and vibrations of the C-Aryl bond at 1300-1360 cm^{-1} [19].

In the spectra of TEOS matrix sample, the C=O vibration mode of Rh B can be observed at the same wavenumber 1742 cm^{-1} no matter of the pH value. In case of MeTEOS-TEOS powders, this peak can slightly be observed at 1746 cm^{-1} in the as prepared sample and becomes more pregnant for the pH 2 and 12 matrices. The band at 1629 cm^{-1} and 1636 cm^{-1} of the TEOS and MeTEOS-TEOS as prepared samples could show the presence of a rhodamine cation of the HR^+ type. For the samples in acid and alkaline conditions the band at ~ 1740 cm^{-1} as well as the disappearance of the ~1630 cm^{-1} band characteristic for HR^+ could be consistent with the formation of a lactone [19].

The PhTEOS-TEOS as-prepared samples show no carboxyl band, but v (C=O) peak can be identified in the spectra of pH 2 and 12 matrices, at 1740 cm^{-1}. There is no band characteristic for the carbocation in any of the three phenyl derived sample.

The presented data suggest that as a function of the matrices and pH, several structural interconversions of the dye take place: cationic form↔zwitterion↔lactone. The lactone is generated at pH 2 and 12 for TEOS and MeTEOS-TEOS samples and in case of PhTEOS-TEOS for the as prepared sample, the acid and basic powder. That could mean a decrease of fluorescence as will be further shown. But the fact that there is no total loss of colour and fluorescence which would be characteristic for the lactone suggests that there is an equilibrium mixture of the tautomers of variable proportion [19].

The 1200-500 cm^{-1} domain shows main characteristic bands of the silica network in all three samples: peaks at about 1100, 800 and 450 cm^{-1} generally due to Si-O-Si stretching and rocking vibrational modes [15,17, 23] can be noticed. In the spectra of TEOS matrix the splitting of the Si-O-Si stretching vibration at pH 2 and 12 into a longitudinal optic mode (LO) at 1207 cm^{-1} and a transversal optic mode (TO) at 1055 cm^{-1} can be a proof of the interactions of silica network with the Rh B [15].

Comparing the matrices colloidal SiO_2-TEOS-(Me) and phenyl (Ph) substituted TEOS, Si-O-Si bands are shifted to lower wavenumbers in the order colloidal SiO_2 (1067 cm^{-1}), TEOS (1055 cm^{-1}), Ph-TEOS (1033 cm^{-1}), Me-TEOS (1024cm^{-1}) indicating a decrease in the bond energy and an increase in the Si-O-Si bond distance. This can be due to the fact that the organosilane gels represent a more open structure with lower cross-linking [15].

Considering the above presented facts one can assume that the interaction of the dye with the alkoxide silica matrices influences its structure and performances in the presence of the variable pH analyte. In this case as in case of colloidal SiO_2 the existence of ionic dye species in aqueous solutions can lead to aggregation [24] confirming the UV-vis results.

3.4.SEM analysis

Figure 2 shows SEM micrographs on a hybrid sample, the PhTEOS-TEOS-Rh B matrices, at pH 2 (Fig. 2A) and pH 12 (Fig. 2B). The influence of pH on the structure of the more densified and hydrophobic form, the Ph substituted matrices, is observed. It can be seen that at pH 2, the PhTEOS-TEOS-Rh B particles are especially polydispersed spheres which aggregate while at pH 12, the shape of PhTEOS-TEOS-Rh B particles is changed and the particles become monodisperse. No loss of sphericity is observed, sign that in a basic environment the sol-gel matrix does not seem to be much perturbed.

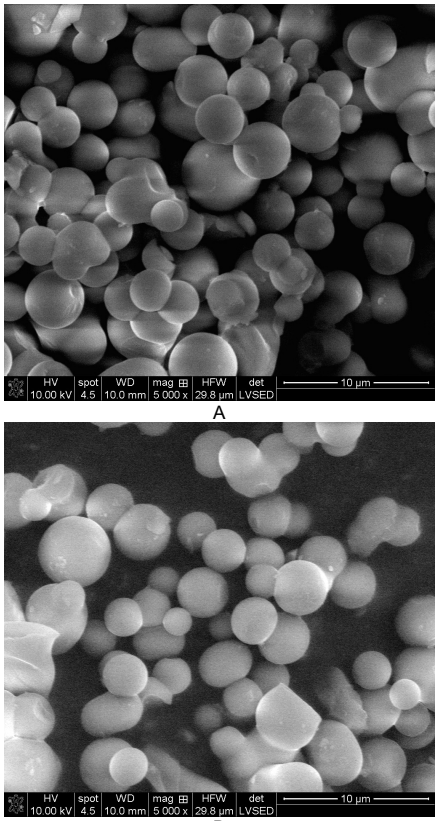

Fig. 2 - SEM micrographs of PhTEOS-TEOS-Rh B at pH 2 (A) and pH 12 (B) */ Micrografii SEM ale PhTEOS-TEOS-Rh B la pH 2 (A) şi pH 12 (B).*

3.5. Fluorescence characteristics of the matrices embedding rhodamine B vs. pH

To get new insights on the mentioned Rh B-matrices as a function of pH, fluorescence spectroscopy was used to monitor the Rh B fluorescence changes.

Previously, we reported [16] the fluorescence emission of the Rh B in three different as prepared matrices: TEOS, MeTEOS-TEOS and PhTEOS-TEOS, for an excitation wavelength of λ_{ex} = 510 nm. The fluorescence emission of Rh B in TEOS and MeTEOS-TEOS, shows an emission maxima at λ_{em}=575 nm, attributed to the monocation form of (HR^+) [25]. A slight decrease was observed in the fluorescence intensity of Rh B in MeTEOS-TEOS matrix and the feature is due to the $–CH_3$ group from the matrix structure that generates a quenching in the fluorescence emission of Rh B. In PhTEOS-TEOS matrix, the Rh B fluorescence emission is strongly quenched with a red-shifted fluorescence emission, λ_{em}=585 nm, showing the formation of a coordination Rh B-phenyl matrix [26]. Also, the higher hydrophobicity of the phenyl group is considered.

At the same excitation wavelengh, Fig. 3A presents the fluorescence emission spectra of Rh B in TEOS matrix, at different pH, pH 2 ÷ 12. It was observed that at low pH, pH 2, the fluorescence intensity of Rh B strongly decreases and the fluorescence emision is 6 nm red-shifted, λ_{em} = 581 nm. Between pH 4.93 ÷12, the fluorescence intensity of Rh B also decreases, the fluorescence emission is blue-shifted, at λ_{em} ~ 572 nm. In direct comparison, Figs. 3B and 3C, show the fluorescence emission of Rh B in Methyl and Phenyl-TEOS-TEOS matrix as a function of pH. In MeTEOS-TEOS matrix (Fig. 3B), the fluorescence intensity of Rh B decreases at low pH, pH 2, with a red-shifted fluorescence emission, λ_{em} =579 nm. For pH 4.93÷12, its fluorescence intensity increases more significantly and the fluorescence emission wavelength is blue-shifted, λ_{em} ~565 nm. In PhTEOS-TEOS matrix (Fig. 3C), the fluorescence emission of Rh B slightly decreases with pH and no changes in the fluorescence emission wavelength, λ_{em} = 585 nm, was observed. With pH increasing, the fluorescence intensity of Rh B increases and the emission wavelength is blue-shifted, λ_{em} = 573 nm. Comparatively, Fig. 3D shows the fluorescence emission spectra of Rh B in colloidal SiO_2, at pH 2 and pH 12. At both pH values, the fluorescence quenching of Rh B in colloidal SiO_2 matrix with a 5 nm blue-shifted emission (λ_{em}=565 nm) at pH 12, were observed. This feature is due to Rh B aggregates.

Figure 4 shows fluorescence excitation spectra of as prepared alkoxide-Rh B matrices (Fig. 4A), PhTEOS-TEOS-Rh B matrice at pH 2 and pH 12 (Fig. 4B) and colloidal SiO_2-Rh B matrice (Fig. 4C), for an emission wavelenght of

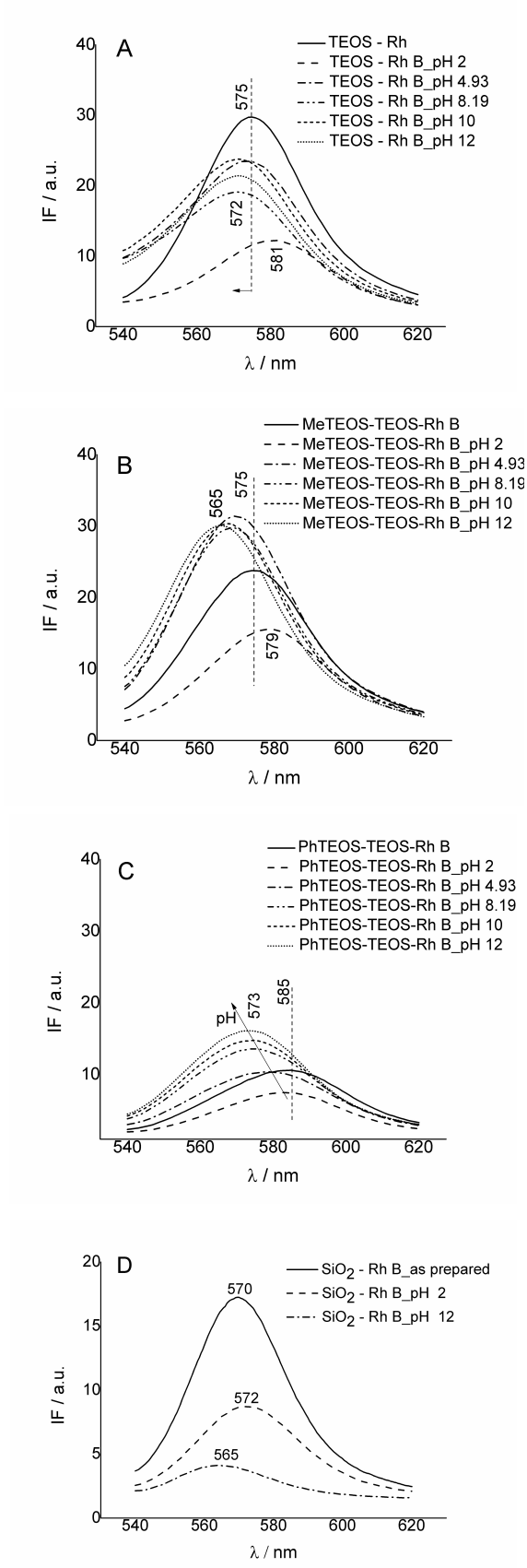

Fig. 3 - Fluorescence emission spectra of Rh B in TEOS (A), MeTEOS-TEOS (B), PhTEOS-TEOS matrice (C) and SiO_2 matrice (D), *vs.* pH; λ_{ex} = 510 nm / *Spectre de emisie de fluorescenţă ale Rh B în următoarele matrici: TEOS (A), MeTEOS-TEOS (B), PhTEOS-TEOS (C) şi SiO_2 (D), funcţie de pH; λ_{ex} = 510 nm.*

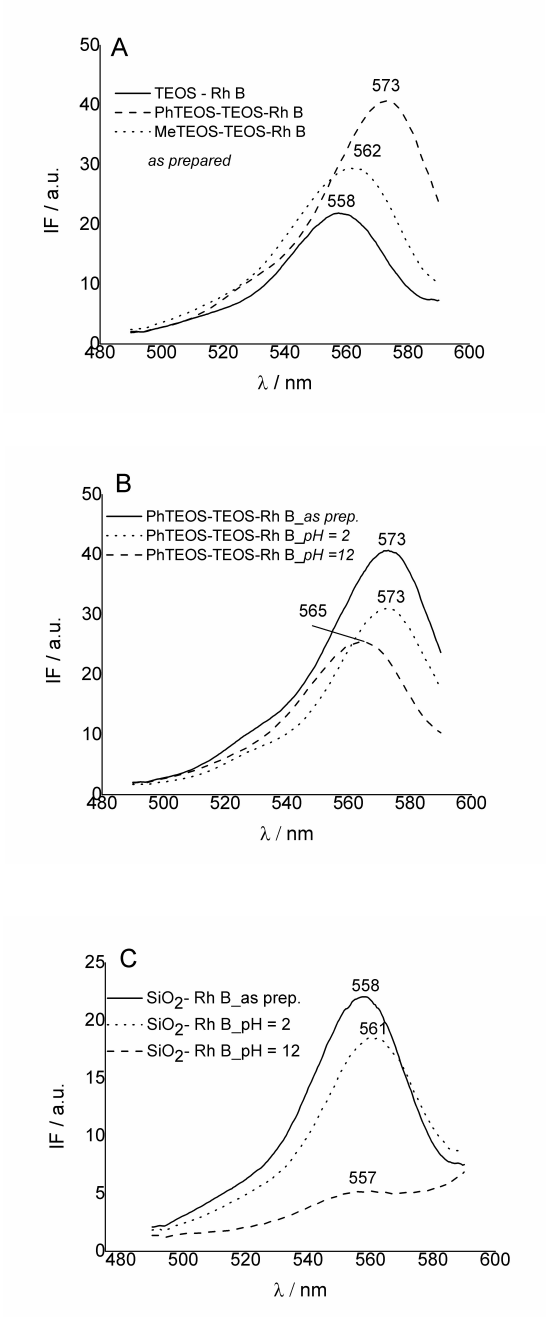

Fig. 4 - Fluorescence excitation spectra of as prepared Rh B matrices (A), PhTEOS-TEOS-Rh B matrix at pH 2 and pH 12 (B) and SiO_2-Rh B matrix (C); λ_{em} = 600 nm / *Spectre de excitație de fluorescență ale următoarelor matrici: preparate ca atare – Rh B (A), PhTEOS-TEOS-Rh B la pH 2 şi pH 12 (B) şi SiO_2-Rh B (C); λ_{em} = 600 nm.*

λ_{em} = 600 nm. One structured absorption band of Rh B (λ_{abs}= 557 - 573 nm) in all studied matrices was observed.

Overall, the fluorescence intensity of Rh B in different alkoxide matrices, at various pH (2 ÷ 12) increases, such as: MeTEOS-TEOS > TEOS > PhTEOS-TEOS. Also, the maximum emission wavelength of Rh B were shown to be dependent on matrix structure and pH. At pH 4.93 ÷ 12, the MeTEOS-TEOS matrix allows a deprotonation of the COOH – group from the Rh B structure leading to its zwitterion structure and thus slight increase in the Rh B fluorescence takes place, more rapidly than the one in PhTEOS-TEOS matrix. At low pH, pH 2, in PhTEOS-TEOS matrix, the monocation form of the Rh B, (HR^+), is more rapidly protonated (than in TEOS and MeTEOS-TEOS matrix) to the dication form, (RH_2^{2+}), with a very weak fluorescence emission.

3.6. Determination of leaching of the dye from the matrices

In contrast to the hybrid composite powders, in case of the colloidal SiO_2 matrix, the leaching of the dye was observed by naked eye due probably to a larger pore size or to the fact that being more polar than alkoxide samples there is a greater interaction with the solution, especially at alkaline pH.

For the alkoxide silica particles, the leaching of Rh B from the matrices was tested by determining the dye presence in the solution used for pH variation by GC-MS, Selected Ion Monitoring method.

A full scan mass range of Rh B was obtained. Rh B fragment ions were chosen for comparison, the highest peak 427, the protonated molecular ion 443, and fragment ion 399, the later being mentioned in literature as key ions [27]. The solutions were analysed by comparison with those ions. No match was found in the chromatograms of the solutions collected from each of the three samples. That could be due to the small porosity (TEOS and MeTEOS-TEOS samples), respectively lack of porosity (PhTEOS-TEOS powder), or to the interaction Rh B-matrix.

4.Conclusions

The present study has shown that the precursor and the sol-gel route has an impact on the final characteristics of the material. Interactions Rh B-silica matrices were evidenced by FTIR , UV-VIS diffuse reflectance spectra, and fluorescence spectroscopy.

These interactions influence the structural interconversions of Rh B which result in a different equilibrium mixture of tautomers. Ionic Rh B species can aggregate. Thus the fluorescence emission performances in the presence of the variable pH analyte change according to the nature of the embedding matrix.

In case of alkoxide samples, TEOS substitution with organic moieties leads to a quenching of fluorescence emission, more pregnant in case of Ph substitution. TEOS particles show a decrease of fluorescence at acid as well as basic pH, while for the Me and Ph derived powders the fluorescence decreases at

low pH and increases with the increase of pH.

A fluorescence quenching of the dye in the colloidal silica matrix at pH 2 and 12 was observed.

The SEM micrographs of PhTEOS-TEOS-Rh B show that a basic environment does not perturb much the hydrophobic embedding matrix. For the alkoxide silica particles no leaching of the dye was registered by GC-MS while in case of colloidal silica powders the leaching of Rh B was visible.

REFERENCES

1. B. D. MacCraith, C. McDonagh, Enhanced fluorescence sensing using sol-gel materials, J. Fluoresc., 2002,**12** (3/4), 333
2. T. Nedelčev, D. Račko, I. Krupa, Preparation and characterization of a new derivative of rhodamine B with an alkoxysilane moiety, Dyes Pigments, 2008, **76**, 550
3. Q.Yang, H. Wang, X. Lan, B. Cheng, S. Chen, H. Shi, H. Xiao, Y. Ma, Reflection-mode micro-spherical fiber-optic probes for in vitro real-time and single-cell level pH sensing, Sensors Actuat B-Chem., 2015**, 207***,* 571
4. S. Dash, S. Mishra, S. Patel, B. K. Mishra, Organically modified silica: synthesis and applications due to its surface interaction with organic molecules, Adv. Colloid Interface Sci., 2008, **140,** 77
5. E. Hwang, I. A.Levitsky, W. B. Euler, Gas Phase Sensors for Bases Using Rhodamine B in Nafion Films, J. Appl. Polym. Sci**.,** 2010**, 116,** 2425
6. A. V. Deshpande, U. Kumar, Effect of higher protonation on lasing performance of Rhodamine-B in sol–gel glasses, J. Non-Cryst. Solids, 2009, **355**, 501
7. M. Formica, V. Fusi, L. Giorgi, M. Micheloni, New fluorescent chemosensors for metal ions in solution; Review, Coord. Chem. Rev., 2012, **256**,170
8. L. Liu, S. Creten, Y. Firdaus, F. Cuautle, J. J. A. Kouyaté, M. Van der Auweraer, M. G. Christ, Fluorescence spectra shape based dynamic thermometry, Appl. Phys. Lett., 2014, 104 (3), 1
9. J. Tu, N. Li, Y. Chi, S. Qu, C. Wang, Q.Yuan, X. Li, S. Qiu, The study of photoluminescence properties of Rhodamine B encapsulated in mesoporous silica, Materials Chemistry and Physics, 2009, **118***,* 273
10. L. B. Capeletti, F. L. Bertotto, J. H. Zi. Dos Santos, E. Moncada, M. B. Cardoso, The effect of the sol–gel route on the characteristics of acid–base sensors, Sens. Actuators, B, 2010,**151,** 169
11. A. Anedda, C. M. Carbonaro, R. Corpino, P. C. Ricci, S. Grandi, P. C. Mustarelli, Formation of fluorescent aggregates in Rhodamine 6G doped silica glasses, J. Non-Cryst. Solids**,** 2007, **353**, 481
12. A. Anedda, C. M. Carbonaro, F. Clemente, R. Corpino, S. Grandi, A. Magistris, P. C. Mustarelli, Rhodamine 6G – SiO2 hybrids: a photoluminescence study, J. Non-Cryst. Solids, 2005, **351***,* 1850
13. M. T. Laranjo, V. Stefani, E. V. Benvenutti, T.M.H. Costa, G. de O. Ramminger, M.R. Galas, Synthesis of ORMOSIL silica/rhodamine 6G: Powders and compacts, J. Non-Cryst. Solids**,** 2007**, 353**, 24
14. M. Gugliemi, G. Brusatin, G. Della Giustina, Hybrid glass-like films through sol-gel techniques, J. Non-Cryst. Solids**,** 2007, **353**, 1681
15. B. Scyrr, S. Pasche, E. Scolan, R. Ischer, D. Ferrario, J-A. Porchet, G. Voirin, Development of a polymer optical fiber pH sensor for on-body monitoring application, Sens. Actuators, B**,** 2014, **194**, 238
16. L. Todan, M. Voicescu, D. C. Culita, C. Stan, S.G. Nitu, V. Marinescu, Performances of hybrid silica-rhodamine B composite particles in Cu^{+2} detection, in press, Rev Roum Chim., 2017, **62(**12**),** 915
17. L. Todan, C. Andronescu, D. M. Vuluga, D. C. Culita, M. Zaharescu, Thermal behavior of silicophosphate gels obtained from different precursors, J. Therm. Anal. Calorym**,** 2013, **114,** 91
18. L. B. Capeletti, I. M. Baibich, I. S. Butler, J. H. Z. Dos Santos, Infrared and Raman spectroscopic characterization of some organic substituted hybrid silicas**,** Spectrochim. Acta A**,** 2014, **133,** 619
19. N.O. Mchedlov-Petrosyan, L.A. Fedorov, S.A. Sokolovskii, Y. N. Surov, M. R. Salinas, Structural conversions of rhodamines in solution, Bulletin of the Russian Academy of Sciences, Division of Chemical Science, 1992, **41**(3), 403
20. J. Coates, Interpretation of infrared spectra, a practical approach, in: Encyclopedia of Analytical Chemistry*,* (Eds.: R.A. Meyers), John Wiley & Sons Ltd, Chichester, 2000**,** pp 10815-10830
21. A. A. M. Farag, I. S. Yahia, Structural, absoption and optical dispersion characteristics of rhodamine B thin films prepared by drop casting technique, Opt. Commun., 2010, **283**, 4310
22. J-Y. Li, W-H. Ma, P-X. Lei, J-C. Zhao, Detection of intermediates in the TiO_2-assited photodegradation of Rhodamine B under visible light irradiation, J. Environ. Sci., 2007**, 19***,* 892
23. P. P. Gan, S. F. Y. Li, Efficient removal of Rhodamine B using a rice hull-based silica supported iron catalyst by Fenton-like process, Chem. Eng. J., 2013, **229***,* 351
24. X. Zhao, S. Zhou, M. Chen, L. Wu,Supramolecular architecture, spectroscopic properties and stability of C.I. Basic Violet 10 (Rhodamine B) at high concentrations, Dyes and Pigments**,** 2009, **80***,* 212
25. R. W. Ramette, E. B. Sandell, Visible and ultraviolet absoption spectra of rhodamine B in aqueous solution, J. Am. Chem. Soc., 1956**, 78**(19)**,** 4872
26. Y.Hua, C.Wang, J. Liu, B.Wang, X. Liu, C.Wu, X. Liu, Visible photocatalytic degradation of Rhodamine B using Fe(III)-substituted phosphotungstic heteropolyanion, J. Mol. Catal. A: Chem., 2012, **365***,* 8.
27. T. Reyns, C. Belpaire, C. Geeraerts, J.Van Loco, Multi-dye residue analysis of triarylmethane, xanthene, phenothiazine and phenoxazine dyes in fish tissue by ultra-performance liquid chromatography- tandem mass spectrometry, Journal of Chromatography B, 2014, **953-954**, 92.

****